

---

# International Journal on Robotics, Automation and Sciences

---

---

## Prostate Cancer Classification Based on Histopathological Images

Nalson Mark a/l Loorutu\*, Haniza Yazid, Khairul Shakir Ab Rahman

**Abstract** - Prostate cancer is a significant health concern, ranking as the third most common cancer in Malaysian men, with increasing incidence in Asia. The importance of automating the prostate cancer classification process lies in its potential to significantly improve diagnostic accuracy, reduce subjectivity, and enhance overall efficiency compared to the manual approach. The objective of this thesis is two-fold: firstly, to effectively enhance and segment crucial features in the images to aid in the classification process, and secondly, to implement a binary classification task that indicates the presence or absence of malignant tissue on histopathology images. The study compares the performance of two image enhancement approaches, stain normalization with adaptive histogram equalization (AHE) and sharpening, and stain normalization with traditional histogram equalization (HE) and sharpening. Additionally, three machine learning models, namely SVM, DenseNet121, and InceptionResNetV2, are implemented and evaluated for prostate cancer binary classification. The findings reveal that AHE contributes to better contrast enhancement and image quality preservation. Moreover, the InceptionResNetV2 model demonstrates superior performance in terms of accuracy (97.25%), sensitivity (97.5%), specificity (97.5%), and area under the curve (AUC) (97.5%).

**Keywords**—Prostate Cancer, Image Processing, Histopathology Images, Digital Image Analysis, Artificial Intelligence.

### I. INTRODUCTION

Prostate cancer, ranked as the third most common cancer among men in Malaysia, presents varying prevalence across different ethnic groups [1]. While the incidence in the country remains relatively low, the overall incidence of prostate cancer is on the rise in Asia, contributing significantly to global prostate cancer-related deaths [2]. The accurate diagnosis and classification of prostate cancer are critical for determining appropriate treatment strategies.

Histopathology images play a pivotal role in diagnosing prostate cancer, offering insights into the microscopic structure of prostate tissue. However, manual interpretation of these images introduces challenges, such as interobserver and intraobserver variability, impacting the reliability of prostate cancer screening and detection [3], [4], [5]. Intraobserver variability is due to the differences in the interpretation of the same tissue sample by the same pathologist, while interobserver variability is due to the differences in the

\*Corresponding author. Email: [nalsonmark349@gmail.com](mailto:nalsonmark349@gmail.com), ORCID: 0000-0003-1760-2473

Nalson Mark a/l Loorutu is with Faculty of Electronic Engineering & Technology, Universiti Malaysia Perlis, Pauh Putra Campus, 02600 Perlis, Malaysia (e-mail: [nalsonmark349@gmail.com](mailto:nalsonmark349@gmail.com)).

Dr. Haniza Yazid is with Faculty of Electronic Engineering & Technology, Universiti Malaysia Perlis, Pauh Putra Campus, 02600 Perlis, Malaysia (e-mail: [hanizayazid@unimap.edu.my](mailto:hanizayazid@unimap.edu.my)).

Dr. Khairul Shakir Ab Rahman is with Hospital Tuanku Fauziah, 01000 Perlis, Malaysia. (e-mail: [ksyakir@gmail.com](mailto:ksyakir@gmail.com)).

International Journal on Robotics, Automation and Sciences (2023) 5,2:43-53

<https://doi.org/10.33093/ijoras.2023.5.2.5>

Manuscript received: 1<sup>st</sup> May 2023 | Revised: 30<sup>th</sup> July 2023 | Accepted: 21<sup>st</sup> August 2023 | Published: 30 September 2023

© Universiti Telekom Sdn Bhd.

Published by MMU PRESS. URL: <http://journals.mmupress.com/ijoras>

This article is licensed under the Creative Commons BY-NC-ND 4.0 International License

interpretation of the same tissue sample by different pathologists.

These variations can lead to inconsistencies in diagnosis and treatment, which can have serious consequences for patients. This not only compromises the individual's well-being but also places a strain on the healthcare system as a whole, necessitating additional resources for corrective measures and potential legal ramifications. The gravity of these consequences emphasizes the urgent need for advanced and reliable techniques that mitigate the impact of manual interpretation challenges.

In light of these challenges, this research project aims to address the need for more accurate and consistent prostate cancer diagnosis. The objectives are twofold: firstly, to enhance and segment essential features in histopathology images, facilitating the classification process; and secondly, to implement a binary classification task to identify the presence or absence of malignant tissue in prostate histopathology images. By achieving these objectives, this project intends to mitigate the challenges posed by manual interpretation and contribute to improved patient outcomes.

The conventional staining method used in pathological biopsies may result in limited distinction between different tissue components, affecting the accuracy of diagnosis. Moreover, pathologists' assessments are influenced by their individual experiences, leading to variability in interpretations [4]. Additionally, the manual analysis of numerous histological images is time-consuming and may lead to misdiagnoses. The scarcity of specialized pathologists further exacerbates the situation [5].

To overcome these challenges, a computer-aided diagnosis (CAD) system is implemented for detecting prostate cancer in histopathological images. The CAD system aims to reduce misdiagnosis rates and provide a valuable second opinion to assist pathologists in their evaluations. The integration of advanced image processing techniques and machine learning algorithms aims to enhance the accuracy and efficiency of prostate cancer diagnosis, ultimately leading to improved patient outcomes.

What sets this research apart is its innovative approach to addressing the diagnostic challenges inherent in histopathological interpretation. By leveraging advanced image processing techniques and state-of-the-art machine learning algorithms, this project presents a novel solution that enhances the reliability and accuracy of prostate cancer classification. Through a combination of image enhancement, and binary classification, this project not only contribute to the technical advancement of the field but also offer a practical tool for healthcare professionals to make more informed decisions.

With a focus on processing 4000 digitalized histopathology prostate cancer images at 40x magnification using Google Colab, the research employs machine learning algorithms, specifically Support Vector

Machine (SVM) and Convolutional Neural Networks (CNNs), for classifying normal and cancerous prostate tissues based on the processed histopathology images.

As we delve into the existing body of research, the subsequent literature review will comprehensively explore state-of-the-art methods and techniques that have been developed to tackle the challenges highlighted in our introduction. By examining the advancements in image enhancement, feature extraction, and deep learning approaches, this project aims to build upon the foundation of knowledge and contribute to the ongoing progress in prostate cancer classification based on histopathological images. With a strong understanding of the existing landscape, we can position this research within the context of these approaches and identify opportunities for further innovation.

## II. LITERATURE REVIEW

Histopathological image analysis plays a pivotal role in the accurate and timely diagnosis of prostate cancer, a prevalent and critical health concern affecting men worldwide. The advancements in medical image processing and machine learning techniques have provided promising avenues for enhancing the classification of prostate cancer based on histopathological images. This literature review presents a comprehensive analysis of state-of-the-art methods and techniques employed in prostate cancer classification, with a specific focus on image enhancement, feature extraction, and deep learning approaches.

### A. Image Enhancement Methods

Image enhancement techniques are of paramount importance in enhancing the quality and visual clarity of histopathological images for subsequent analysis and interpretation. These techniques encompass various methods, including image sharpening, contrast adjustment, and stain normalization, which collectively enhance image quality, accentuate crucial details, and eliminate artefacts that might impact subsequent analyses. Among the commonly employed techniques, noise reduction plays a vital role in mitigating noise in histopathological images caused by factors such as image acquisition, staining variations, and digitization processes. By effectively reducing noise, image enhancement ensures that critical information is not obscured, enabling accurate interpretations and classifications. Gaussian filtering [6], median filtering [7], and wavelet-based [8] methods are frequently utilized to reduce noise while preserving essential image details. Studies by Xuru [6] highlighted the efficacy of Gaussian filtering in preserving edge contour information, resulting in improved model learning and enhanced classification accuracy.

Contrast adjustment is equally crucial and involves modifying intensity levels to enhance the visual distinction between structures or components. Techniques like histogram equalization [9], [10], [11], adaptive histogram equalization [10], [11], and contrast

stretching [11] enhance the visibility of significant features within histopathological images. Notably, Acharya's [8] adaptive image enhancement technique utilizing genetic algorithms demonstrated remarkable results in various metrics, making it promising for disease interpretation and diagnosis.

Stain normalization techniques are essential for standardizing colour appearance across different histopathological images, thus ensuring consistent analysis and interpretation. The widely used Macenko and Reinhard approach successfully normalizes the colour of histopathological images, facilitating better tissue recognition and classification by machine learning models [12], [13]. Ultimately, the application of these enhancement techniques enhances the accuracy and reliability of histopathological image analysis, with the selection of specific methods contingent on image characteristics and analysis requirements.

#### *B. Feature Extraction using Local Binary Patterns (LBP)*

Feature extraction is a critical step in histopathological image analysis, aiming to capture relevant information for subsequent analysis and classification tasks. Texture analysis, a commonly employed technique, quantifies spatial arrangements and pixel intensity variations to provide insights into tissue patterns and structures. One widely used method for texture analysis is Local Binary Patterns (LBP), which encodes local texture patterns by comparing each pixel's intensity value with the values of its neighboring pixels. Specifically, LBP assigns a binary code to each pixel based on whether its intensity is greater than or less than the intensity of the surrounding pixels. This process captures variations in texture, such as edges, corners, and other patterns. Gray-level co-occurrence matrices (GLCM) [14] and Gabor filters [15] are also frequently used for texture feature extraction. Öztürk et al. [14] investigated the use of GLCM and LBP, finding that the GLCM-based approach achieved the highest accuracy of 98.33% for tissue type identification. When combined with GLCM and other methods, LBP yielded the highest classification accuracy for histological tissue images. Gabor filters, which analyze frequency and orientation components, have been widely used for tissue classification, tumor detection, and grading, achieving an impressive 95.8% accuracy in binary classification. Shape analysis, another crucial method, focuses on geometric characteristics and contours of objects in histopathological images, providing valuable information about structural irregularities and morphological changes [16], [17]. The choice of feature extraction techniques depends on analysis objectives and image characteristics, with the extracted features serving as input for subsequent classification algorithms to develop robust and accurate models for histopathological image analysis.

#### *C. Convolutional Neural Networks (CNNs)*

In recent years, deep learning architectures, particularly Convolutional Neural Networks (CNNs), have demonstrated remarkable performance in various

medical image analysis tasks, including prostate cancer classification. CNNs are designed to automatically learn hierarchical features from images by applying convolutions and pooling operations that progressively extract low- to high-level features. This enables them to capture complex patterns and structures effectively. Numerous studies have explored the application of CNNs for prostate cancer classification based on histopathological images. For instance, Karimi et al. [18] proposed a deep learning-based method that achieved high classification accuracies, comparable to expert pathologists, demonstrating the potential of well-designed deep learning models in Prostate Cancer Gleason grading. Similarly, Gour et al. [19] compared various state-of-the-art CNN models and found that the EfficientNet-B7 model showed promise as a valuable tool for pathologists in determining the stage of prostate cancer. Kott et al. [20] developed a state-of-the-art deep learning algorithm using ResNet, achieving high accuracy in classifying image patches and Gleason grading of prostate biopsy specimens. Tolkach et al. [21] presented DL-based models using the NASNetLarge architecture, achieving high accuracy in the detection of prostate cancer tissue and Gleason grading. Jusman et al. [22] conducted a study on prostate cancer cell detection using pre-trained deep learning models, demonstrating good performance in classifying prostate images. The review also highlights the potential applicability of CNN models in classifying breast cancer in histopathological images, as demonstrated by Al-Haija et al. [23], Motlagh et al. [24], and Parvin et al. [25]. These studies collectively showcase the promising role of deep learning in enhancing the accuracy and efficiency of cancer diagnosis, offering possibilities for advancements in medical image analysis. Recent advancements in CNNs, including residual connections, attention mechanisms, transfer learning, hardware improvements, and regularization techniques, have significantly contributed to their improved performance in various computer vision applications.

#### *D. Support Vector Machines (SVM)*

Machine learning algorithms, such as support vector machines (SVM), random forests, and k-nearest neighbors (KNN), have gained widespread popularity in the classification of prostate cancer using histopathological images. SVM, particularly esteemed for its ability to manage high-dimensional feature spaces and its effectiveness in binary classification tasks, has been extensively employed in this domain. SVM functions by finding the optimal hyperplane that best separates different classes of data points. This hyperplane maximizes the margin between the two classes, allowing SVM to make accurate predictions for new, unseen data points. For instance, Bhattacharjee et al. [26] achieved an accuracy of 88.7% in prostate cancer classification using SVM on histopathological images.

However, ongoing research aims to enhance SVM's accuracy by combining multiple features and integrating deep learning techniques such as Convolutional Neural Networks (CNNs). Notably, SVM's applicability extends

beyond prostate cancer, as demonstrated in breast cancer classification. Aswathy and Jagannath [27] introduced an integrated SVM model for breast cancer classification, achieving an accuracy of approximately 90%. Alqudah et al. [28] utilized LBP features with a sliding window-based SVM system, achieving an overall accuracy of 91.12% in breast cancer classification. Singh et al. [29] proposed a cubic SVM classifier for breast cancer detection and classification, achieving a peak accuracy of 92.3%. Additionally, Lopez et al. [30] developed a clinical decision support tool incorporating SVM, naïve Bayes, and KNN classifiers, where SVM outperformed others with an accuracy of 0.7490 in detecting invasive ductal carcinoma.

While SVM boasts robustness, it does have limitations, including sensitivity to noisy data, computational expense for large datasets, and intricate model interpretation. Nonetheless, advancements like kernel tricks and stochastic gradient descent optimization have bolstered SVM's performance. The integration of deep learning architectures like CNNs has further augmented SVM's capabilities in handling complex data and achieving state-of-the-art results.

#### E. Performance Evaluation

The evaluation of these methods involves the use of various performance metrics to assess their effectiveness. For classification tasks, commonly used metrics include accuracy, sensitivity, specificity, and area under the ROC curve (AUC). Accuracy measures the proportion of correctly predicted instances, sensitivity evaluates the true positive rate, and specificity assesses the true negative rate. AUC provides a comprehensive measure of the model's performance in distinguishing between cancerous and non-cancerous regions.

On the other hand, image enhancement techniques are evaluated using mean squared error (MSE), structural similarity index measure (SSIM), and peak signal-to-noise ratio (PSNR). MSE quantifies the average squared difference between the enhanced image and the original image, with lower values indicating better enhancement. SSIM is a metric that evaluates the structural similarity between the enhanced and original images, measuring the preservation of structures and textures. Higher SSIM values indicate better preservation of image features. PSNR measures the ratio of the maximum pixel value to the mean squared error and indicates the quality of the enhanced image. Higher PSNR values suggest better enhancement quality. These metrics collectively provide valuable insights into the effectiveness of image enhancement techniques in improving the visual quality and interpretability of histopathological images.

Histopathological image datasets present significant challenges in collection and annotation. Expert pathologists are required for manual annotation, which is time-consuming and subjective. Collecting large-scale, well-annotated datasets necessitates collaboration among medical institutions. Moreover, privacy concerns and ethical considerations further complicate the process of dataset acquisition.

#### D. Recent Advancements in 2023

The landscape of prostate cancer classification has seen remarkable advancements in 2023, marked by studies that contribute significantly to the refinement of histopathological image analysis. Among these recent breakthroughs, Fogarty et al. [31] developed a deep learning (DL) model aimed at identifying the most prominent Gleason pattern. Their approach, validated on an independent dataset, effectively discriminates cancer grade from benign tissue, achieving remarkable accuracies of 91% and an AUC of 0.96. Bazargani et al. [32] addressed the domain shift challenge in histopathology image analysis by introducing a novel centre-based H&E colour augmentation technique. This approach enhances the generalization power of deep learning models across datasets from different institutes, demonstrating promise in learning more generalizable features for histopathology image analysis. Moreover, Nishio et al. [33] focused on automatic prediction systems for grading histopathological images using deep learning models and label distribution learning (LDL). Their LDL-enhanced system exhibited improved diagnostic performance for prostate cancer grading, showcasing the potential of novel techniques in enhancing accuracy and reliability in cancer diagnosis.

These recent advancements underscore the continuous evolution of histopathological image analysis, with researchers leveraging innovative methodologies to overcome existing challenges and elevate the accuracy and efficiency of prostate cancer classification.

### III. METHODOLOGY

#### A. Proposed Methodology

The proposed methodology for this study is chosen based on the project's objectives and nature. The primary aim of the project is to develop a robust classification system for prostate cancer using histopathological images. To achieve this, a systematic research design is employed, allowing for the evaluation of various image enhancement techniques to improve the quality and clarity of the images. This approach facilitates the exploration of multiple pathways to achieve accurate classification results.

A flowchart and its pseudocode representing the proposed research design is presented in Figure 1 and Table 1 respectively. The flowchart outlines the sequential steps involved in classifying prostate cancer using histopathological images. It includes image enhancements, feature extraction, and classification using supervised techniques such as Support Vector Machines (SVM) and Convolutional Neural Networks (CNN) – specifically DenseNet121 and InceptionResNetV2. The research design enables a structured approach to address the research objectives and provides a framework for evaluating the proposed methods in the context of prostate cancer classification.

TABLE1. Pseudocode of proposed methodology.

| Pseudocode of Proposed Methodology           |
|--|
| <b>Start</b>                                 |
| Load Prostate histopathological image        |
| <b>Image Enhancement:</b>                    |
| Apply Stain Normalization                    |
| Apply Adaptive Histogram Equalization        |
| Apply Sharpening                             |
| Evaluate Performance                         |
| <b>If</b> Performance is not satisfactory:   |
| Go back to Stain Normalization               |
| <b>Else:</b>                                 |
| Proceed to Classification                    |
| <b>End Image Enhancement</b>                 |
| <b>Classification:</b>                       |
| Supervised (Choose a classification method): |
| <b>If</b> SVM:                               |
| Feature Extraction using LBP                 |
| Classification using SVMs                    |
| <b>Else if</b> CNNs:                         |
| Choose a CNN architecture:                   |
| <b>If</b> DenseNet121:                       |
| Apply DenseNet121 model                      |
| <b>Else if</b> InceptionResnetV2:            |
| Apply InceptionResnetV2 model                |
| Classification using chosen CNN              |
| Evaluate Performance                         |
| <b>If</b> Performance is not satisfactory:   |
| Go back to Supervised                        |
| <b>Else:</b>                                 |
| Proceed to End                               |
| <b>End Classification</b>                    |
| <b>End Start</b>                             |

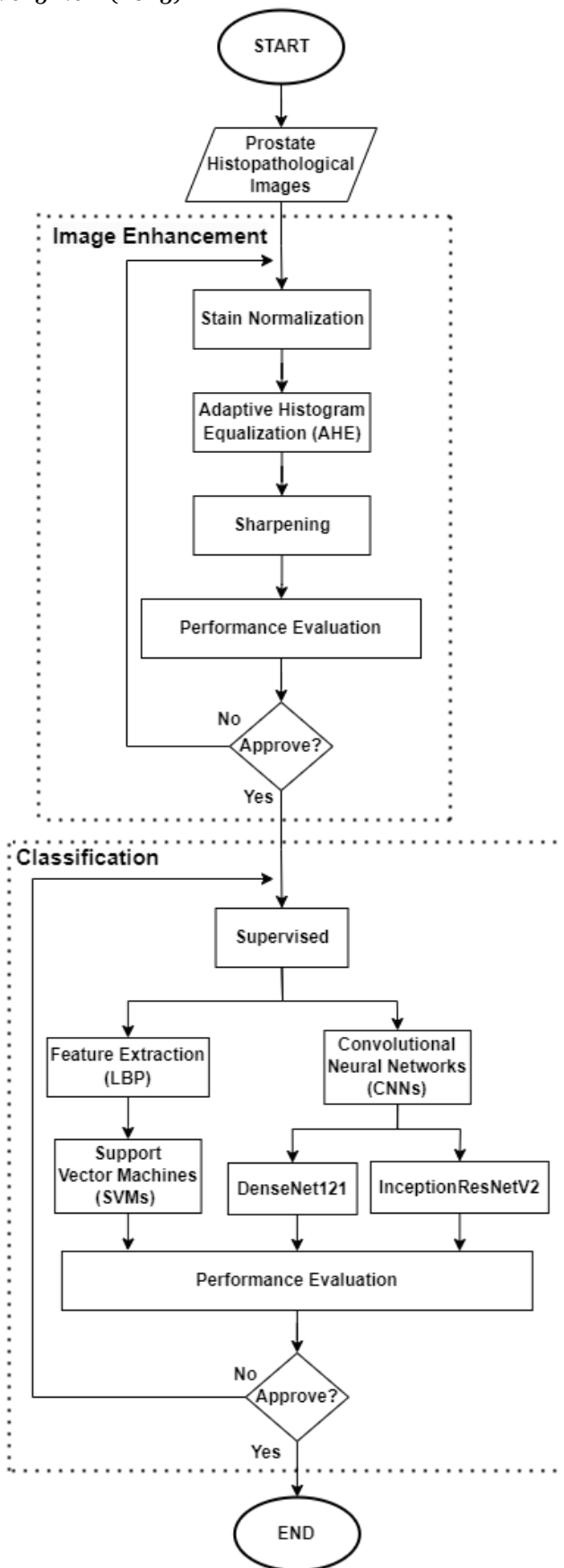


FIGURE 1. Histopathology-Based Prostate Cancer Classification Flowchart.

B. Data Retrieval

The foundation of this research lies in the acquisition and curation of a comprehensive histopathological image dataset meticulously tailored to the study's focus – the accurate classification of prostate cancer. This section details the selection process, considerations, and tools employed for data retrieval and management.

The chosen dataset, known as Diagset-A [34], represents a dedicated repository designed explicitly for prostate cancer detection. It comprises over 2.6 million tissue patches extracted from 430 fully annotated scans, 4675 scans with binary diagnosis, and 46 scans independently diagnosed by histopathologists.

Within this vast dataset, a carefully curated subset of 4000 images was extracted to closely align with the research objectives. These selected images are characterized by their alignment with a 40x magnification, a level that effectively balances granularity and coverage. This selection criterion was grounded in the pursuit of images that preserve intricate cellular details while maintaining a coherent overview of the tissue. The dataset was divided into 80% training dataset and 10% each for validation and testing datasets.

It is important to acknowledge that the original dataset presented certain complexities. Notably, the dataset was initially annotated across nine distinct classes, reflecting various Gleason grades. To mitigate challenges stemming from potential imperfections in the dataset and to streamline in this research, a strategic

decision was made to consolidate the five Gleason grades. This amalgamation ultimately resulted in a binary classification scheme, categorizing tissues as either benign or malignant. This refinement facilitated a more focused and coherent approach to subsequent analysis and classification.

Central to the operational foundation of this study is the utilization of Google Colab, a cloud-based Jupyter notebook environment. Google Colab plays a pivotal role in facilitating data retrieval and management, enabling seamless interaction with the dataset and analysis tools.

The adoption of Google Colab strategically addresses the challenges inherent to managing a dataset of substantial scale. The cloud-based nature of this platform effectively mitigates concerns related to computational resources, fostering agility in data exploration, preprocessing, and manipulation. Furthermore, Google Colab's compatibility with an array of essential Python libraries ensures a harmonious integration of established image processing and analysis techniques.

### C. Image Enhancement

This phase constitutes a pivotal step aimed at elevating the quality and interpretability of a carefully chosen subset of 4000 histopathological images. This segment delves into the meticulous application of three pivotal techniques – stain normalization, histogram equalization (HE), and sharpening. The selection of these techniques was meticulously informed by a comprehensive literature review and further scrutinized through rigorous evaluation employing metrics such as peak signal-to-noise ratio (PSNR), mean squared error (MSE), and structural similarity index measure (SSIM).

#### i. Stain Normalization for Consistency and Quality:

Among the triad of enhancement techniques, stain normalization emerges as a cornerstone. Its core objective revolves around rectifying colour variations inherent in histopathological images, thereby augmenting visual quality and ensuring consistency. The method of choice for stain normalization is the well-regarded Macenko method. This method intricately navigates a series of sequential steps to attain the desired colour transformation.

To execute Macenko's stain normalization within the context of Google Colab, a coherent sequence unfolds:

1. **Convert RGB to Optical Density (OD):** The RGB representation of the image undergoes a transformation into the optical density space, effectively separating colour attributes from intensity information.
2. **Remove Low Intensity Data:** Intensity values below a predefined threshold (B) are pruned, enhancing image clarity by eliminating low-intensity artifacts.
3. **Singular Value Decomposition (SVD) on OD Tuples:** Employing singular value decomposition,

the directions of maximal variance within the optical density space are unveiled.

4. **Construct Plane from SVD Directions:** The two most prominent singular values guide the creation of a plane, encapsulating the predominant colour variations.
5. **Project Data onto Plane and Normalize:** Image data is projected onto the plane, culminating in the normalization of this projection to ensure uniformity.
6. **Calculate Angle of Each Point:** The normalized space is harnessed to compute the angle of every data point in relation to the leading SVD direction, effectively quantifying colour characteristics.
7. **Identify Robust Extremes:** Through percentile analysis, robust angle extremes ( $\alpha^{th}$  and  $(100 - \alpha)^{th}$  percentiles) are discerned, encapsulating the quintessential color characteristics.
8. **Convert Extremes back to OD:** These extreme angle values are meticulously reconverted into optical density space, yielding the optimal stain vectors.

#### ii. Adaptive Histogram Equalization (AHE) for Contrast and Brightness:

The journey of enhancement further embraces Adaptive Histogram Equalization (AHE), an approach meticulously calibrated to amplify contrast and luminosity. AHE extends its reach by adapting transformation functions to the unique properties of discrete tiles within the image. The orchestration of AHE in this project, harmoniously orchestrated within Google Colab, unfolds as follows:

1. **Division into Tiles:** The image canvas is partitioned into non-overlapping tiles or regions.
2. **Histogram Calculation:** Each tile's histogram is meticulously calculated, encapsulating the frequency distribution of pixel intensities.
3. **Independent Transformation:** Individual tiles undergo independent histogram equalization transformations, magnifying contrast and luminosity. The transformation function is founded on a discrete approximation of grey level probabilities, anchored by Equation (1) and (2).
 
$$p_r(r_k) = \frac{n_k}{n} \quad \text{where } k = 0, 1, \dots, L - 1 \quad (1)$$

$$s_k = T(r_k) = (L - 1) \sum_{j=0}^k p_r(r_j) \quad (2)$$
 where  $k = 0, 1, 2, \dots, L - 1$
4. **Tiles Convergence:** The equalized tiles convene, giving rise to an enriched and enhanced image, endowed with augmented contrast and luminosity.

### iii. Sharpening for Edge and Detail Enhancement:

Completing the triumvirate of enhancement techniques is the application of sharpening, executed through the judicious utilization of a Gaussian kernel. This technique embarks on a transformative journey aimed at accentuating edges and finer details. The Gaussian kernel, facilitated through convolution, embraces a dual role – accentuating high-frequency components while steadfastly preserving integral image features. A coherent portrayal of sharpening's orchestration is articulated through the following sequence:

1. **Convolution with Gaussian Kernel:** The original image embarks on a convolutional encounter with a Gaussian kernel, yielding a perceptible shift toward a blurred rendition.

Gaussian kernel:

|      |   |   |   |
|------|---|---|---|
| 1/16 | 1 | 2 | 1 |
|      | 2 | 4 | 2 |
|      | 1 | 2 | 1 |

2. **Blurred Image Subtraction:** The blurred counterpart is meticulously subtracted from the original image, culminating in the extraction of high-frequency constituents intrinsic to edges and finer details.
3. **Amplification of High-Frequency Components:** These high-frequency elements are subjected to an amplification regime, intensifying sharpness and accentuating the prominence of edges.

### D. Image Classification

The conclusive stage of this study entails the meticulous classification of histopathological prostate cancer images via the skilful utilization of supervised classification methodologies. This segment delves into the deployment of Support Vector Machine (SVM) and Convolutional Neural Network (CNN) models, both adapted with precision to realize the objective of precise classification. At the core of this endeavour lies the fundamental principle of supervised classification, whereby labelled data serves as the bedrock upon which predictive models are cultivated, empowering them to uncover patterns and foresee labels for previously unseen instances.

The application of Support Vector Machine (SVM) stands as a pivotal element in the quest for classification accuracy. The journey commences with the extraction of features through the utilization of Local Binary Patterns (LBP), a revered texture descriptor renowned for capturing localized patterns that intricately define an image's texture. This texture-focused perspective provides the foundation upon which SVM, fortified with the Radial Basis Function (RBF) kernel, excels. The RBF kernel confers the SVM with the ability to navigate

complex, non-linear data distributions, thereby facilitating the discernment of intricate patterns.

Parallel to the SVM narrative, Convolutional Neural Networks (CNNs) emerge as potent instruments within the classification repertoire. In this phase, two distinct CNN architectures come into play – DenseNet121 and InceptionResNetV2. Each architecture is meticulously tailored to uncover inherent features and patterns within images. The mechanism adopted is transfer learning, a technique that capitalizes on pre-trained models, refining them to our specific dataset.

- **DenseNet121:** The selection of DenseNet121 is grounded in its ability to reuse features, facilitating the capture of fine-grained intricacies within images. This architecture, characterized by dense connections between layers, heightens the model's capacity to extract nuanced details concealed within images.
- **InceptionResNetV2:** Augmenting the ensemble is InceptionResNetV2, a hybrid architecture amalgamating the strengths of Inception and ResNet models. This amalgamation enriches the learning process, empowering the model to unravel intricate and discriminative features pivotal to classification.

The orchestration of DenseNet121 and InceptionResNetV2, in conjunction with the training and evaluation procedures, unfolds within the nurturing embrace of Keras, while TensorFlow assumes the mantle of the backend. Keras stands as an intuitive arena, seamlessly facilitating the construction and training of intricate deep learning models. Harmonizing with this frontend grace is TensorFlow, an optimization powerhouse that fuels the computation and optimization underpinning expansive neural networks.

## IV. RESULTS AND DISCUSSION

### A. Performance Evaluation of Image Enhancement Techniques

The study evaluated two different approaches for image enhancement in the context of prostate cancer classification. The first approach utilized stain normalization with the Macenko method, followed by adaptive histogram equalization (AHE) and sharpening with a Gaussian filter. The second approach also employed stain normalization with the Macenko method but used traditional histogram equalization (HE) instead of AHE, followed by sharpening with a Gaussian filter. Sample outputs of both approaches are denoted in Figure 2, Figure 3, and Figure 4. The evaluation was based on quantitative metrics such as peak signal-to-noise ratio (PSNR), mean squared error (MSE), and structural similarity index measure (SSIM).

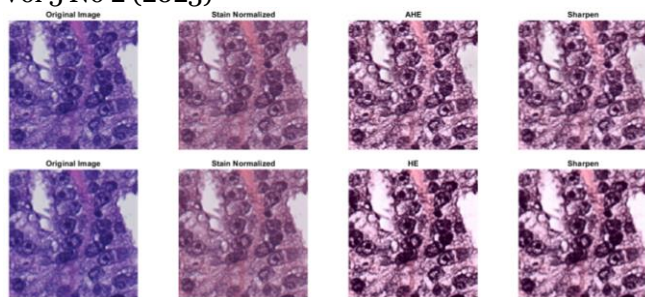


FIGURE 2. Original Image of Cancer Sample 69 with the Two Approaches.

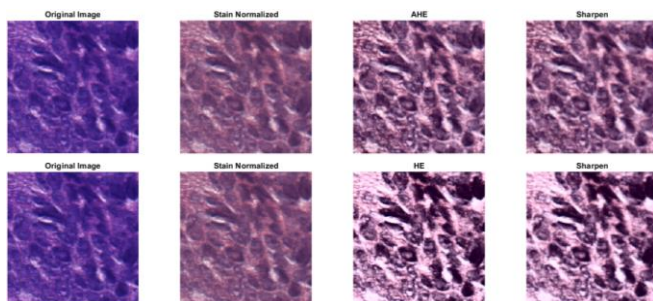


FIGURE 3. Original Image of Cancer Sample 435 with the Two Approaches.

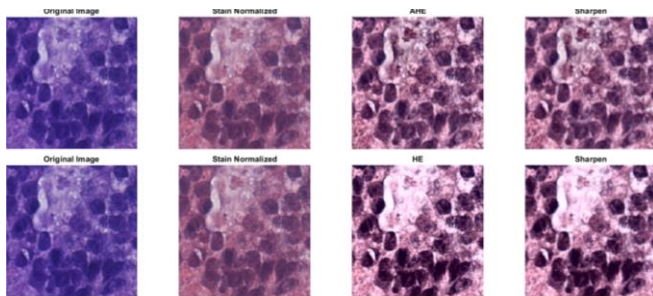


FIGURE 4. Original Image of Cancer Sample 1232 with the Two Approaches.

TABLE 2. Performance Evaluation of Image Enhancement Approaches.

| Approach                               | Average PSNR (dB) | Average MSE | Average SSIM |
|--|-------------------|-------------|--------------|
| Stain Normalization + AHE + Sharpening | 18.7994           | 99.0596     | 0.8381       |
| Stain Normalization + HE + Sharpening  | 15.7363           | 105.0273    | 0.7052       |

The results in Table 2 indicated that the Stain Normalization + AHE + Sharpening approach outperformed the Stain Normalization + HE + Sharpening approach in terms of PSNR, MSE, and SSIM. The first approach achieved a higher average PSNR (18.80 dB) compared to the second approach (15.74 dB), indicating better preservation of image details and less distortion. The Stain Normalization + AHE + Sharpening approach also had a lower average MSE (99.06) compared to the Stain Normalization + HE + Sharpening approach (105.03), implying a closer resemblance between the enhanced and original images. Additionally, the first approach yielded a higher

average SSIM (0.84) compared to the second approach (0.71), signifying better preservation of structural information in the enhanced images.

The findings suggest that AHE contributes to better contrast enhancement and image quality preservation compared to traditional HE when combined with stain normalization and sharpening techniques. The localized approach of AHE allows for more effective contrast enhancement and preservation of image features compared to the global nature of traditional histogram equalization.

TABLE 3. Performance Evaluation of Different Image Enhancement Approaches using InceptionResNetV2.

| Approach                                    | InceptionResNetV2 Model Accuracy (%) |
|---|--------------------------------------|
| Original Dataset                            | 95.00                                |
| Stain Normalized Dataset                    | 92.78                                |
| AHE Dataset                                 | 91.11                                |
| Sharpen Dataset                             | 95.56                                |
| Stain Normalized + Sharpen Dataset          | 93.89                                |
| Stain Normalized + AHE Dataset              | 94.44                                |
| Stain Normalized + Sharpen + AHE Dataset    | 95.08                                |
| Stain Normalization + AHE + Sharpen Dataset | 97.22                                |

Table 3 presents the results of evaluating various image enhancement techniques using the InceptionResNetV2 model for prostate cancer classification. These results provide essential insights into the impact of each approach on the model's accuracy and highlight the rationale for choosing a specific enhancement strategy.

The accuracy of the "Original Dataset" (95.00%) serves as a baseline for evaluating enhancement methods and understanding their effects. The "Stain Normalized Dataset" (92.78%) showcases the efficacy of stain normalization alone, mitigating colour inconsistencies in histopathological images. "Sharpen Dataset" (95.56%) highlights the benefits of image sharpening in capturing finer diagnostic features.

The combined approaches demonstrate nuanced outcomes: "Stain Normalized + Sharpen Dataset" (93.89%) suggests complementary strengths, while "Stain Normalized + AHE Dataset" (94.44%) offers a moderate boost from AHE. Notably, "Stain Normalization + AHE + Sharpen Dataset" achieves the highest accuracy at 97.22%, illustrating the potential of a comprehensive approach.

Hence, the results in Table III underscore the significance of a customized image enhancement pipeline. The sequential application of stain normalization, AHE, and sharpening contributes to substantial accuracy improvements, highlighting the merits of a balanced enhancement strategy. This approach was selected because it demonstrates the most promising outcomes in terms of classification accuracy, providing a robust framework for enhancing histopathological images for prostate cancer classification using InceptionResNetV2.

**B. Prostate Cancer Classification Results and Analysis**

The study employed three classification models for prostate cancer classification: Support Vector Machine (SVM), DenseNet121, and InceptionResNetV2. Each model underwent a thorough parameter tuning process, and data augmentation techniques were applied to enhance generalization capabilities. The models were evaluated using metrics such as accuracy, sensitivity, specificity, and area under the ROC curve (AUC).

**TABLE 4. Performance Evaluation of SVM, DenseNet121, and InceptionResNetV2.**

| Model              | Accuracy      | Sensitivity   | Specificity   | AUC           |
|--------------------|---------------|---------------|---------------|---------------|
| SVM                | 0.8550        | 0.8450        | 0.8650        | 0.9448        |
| DenseNet121        | 0.9600        | 0.9700        | 0.9650        | 0.9675        |
| InceptionResNet V2 | <b>0.9725</b> | <b>0.9750</b> | <b>0.9750</b> | <b>0.9750</b> |

The results in Table 4 showed that all three models achieved high accuracy and AUC values, indicating their effectiveness in prostate cancer classification. The InceptionResNetV2 model outperformed the other two models, achieving the highest accuracy (97.25%), sensitivity (97.50%), specificity (97.50%), and AUC (0.9750). The DenseNet121 model also exhibited strong performance with an accuracy of 96.00%, sensitivity of 97.00%, specificity of 96.50%, and AUC of 0.9675. The SVM model achieved an accuracy of 85.50%, sensitivity of 84.50%, specificity of 86.50%, and AUC of 0.9448.

The superior performance of the InceptionResNetV2 model can be attributed to its ability to capture complex patterns and hierarchies in images through its deep architecture and residual connections. The InceptionResNetV2 model incorporates both the benefits of the Inception module for multi-scale feature extraction and the ResNet architecture for easier training of very deep networks.

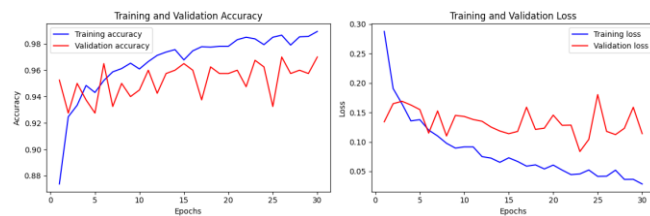


**FIGURE 4. Training and Validation Accuracy-Loss Graph of InceptionResNetV2.**

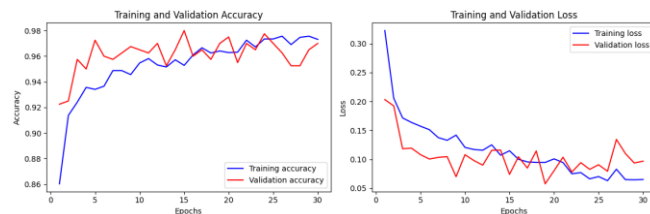


**FIGURE 5. Training and Validation Accuracy-Loss Graph of Densenet121.**

The training and validation accuracy/loss graphs for both DenseNet121 (Figure 5) and InceptionResNetV2 (Figure 4) models demonstrated a positive trend, with accuracy steadily improving over time. Both models exhibited good generalization capabilities, as the validation accuracy closely tracked the training accuracy without overfitting.

The findings of the study align with existing literature, which also demonstrates the effectiveness of deep learning techniques, especially CNNs, in prostate cancer classification based on histopathological images. The inclusion of SVM in the analysis provided a comprehensive evaluation and comparison of different classification techniques.

Overall, the study highlights the potential of deep learning models, particularly InceptionResNetV2, for prostate cancer classification using histopathological images. The high accuracy and AUC values obtained by all three models indicate the effectiveness of deep learning and machine learning techniques in this domain. The study's implementation details and parameter tuning process contribute to the transparency and reliability of the research findings.

**V. CONCLUSION**

In conclusion, this research demonstrates the effectiveness of image enhancement techniques and deep learning models for prostate cancer classification based on histopathological images. The study reveals that stain normalization with adaptive histogram equalization (AHE) and sharpening outperforms stain normalization with histogram equalization (HE) and sharpening in enhancing image quality. Additionally, the InceptionResNetV2 model shows superior performance among Support Vector Machine (SVM), DenseNet121, and InceptionResNetV2, achieving the highest accuracy, sensitivity, specificity, and AUC values. The research provides valuable insights and recommendations for future work, including the use of larger datasets, ensemble models, explainable AI, and integration into clinical practice. These findings contribute to the ongoing efforts in improving prostate cancer diagnosis and treatment, ultimately benefiting patient outcomes both in Malaysia and globally.

**ACKNOWLEDGMENT**

We sincerely thank Dr. Khairul Shakir Ab Rahman from Hospital Tuanku Fauziah for their valuable assistance and our project supervisor, Dr. Haniza Yazid, for their guidance and support. Our heartfelt appreciation also goes to our colleagues and families for their understanding and encouragement throughout this project.

**FUNDING STATEMENT**

No funding was funded for this paper.

## AUTHOR CONTRIBUTIONS

Nalson Mark a/l Loorutu: Conceptualization, Data Curation, Methodology, Validation, Writing – Original Draft Preparation;

Khairul Shakir Ab Rahman: Project Administration, Validation, Writing – Review & Editing;

Haniza Yazid: Project Administration, Supervision, Writing – Review & Editing.

## CONFLICT OF INTERESTS

No conflict of interests were disclosed.

## ETHICS STATEMENTS

Our publication ethics follow The Committee of Publication Ethics (COPE) guideline. <https://publicationethics.org/>

## REFERENCES

- [1] A. A. Manan, H. Basri, N. Kaur, S. Z. A. Rahman, P. N. Amir, N. Ali, S. Raman, B. Bahtiar, N. S. M. Ramdzuan, S. S. S. Soffian, R. Othman, N. A. Othman, and A. A. Aziz, "Malaysia National cancer registry report (MNCR)," 2019. [Online]. Available: [http://www.moh.gov.my/moh/resources/Penerbitan/Laporan/Umum/2012-2016%20\(MNCR\)/MNCR\\_2012-2016\\_FINAL\\_\(PUBLISHED\\_2019\).pdf](http://www.moh.gov.my/moh/resources/Penerbitan/Laporan/Umum/2012-2016%20(MNCR)/MNCR_2012-2016_FINAL_(PUBLISHED_2019).pdf) (Accessed: 19, Jun, 2023).
- [2] H. Sung, J. Ferlay, R.L. Siegel, M. Laversanne, I. Soerjomataram, A. Jemal and F. Bray, "Global Cancer Statistics 2020: GLOBOCAN Estimates of Incidence and Mortality Worldwide for 36 Cancers in 185 Countries," *CA: A Cancer Journal for Clinicians*, vol. 71, no. 3, pp. 209-249, 2021. DOI: <https://doi.org/https://doi.org/10.3322/CAAC.21660>
- [3] D. Karimi, G. Nir, L. Fazli, P. C. Black, L. Goldenberg, and S. E. Salcudean, "Deep Learning-Based Gleason Grading of Prostate Cancer From Histopathology Images – Role of Multiscale Decision Aggregation and Data Augmentation," *IEEE J Biomed Health Inform*, vol. 24, no. 5, pp. 1413–1426, May 2020, DOI: <https://doi.org/10.1109/JBHI.2019.2944643>.
- [4] J. Wang, R. J. Chen, M. Y. Lu, A. Baras, and F. Mahmood, "Weakly Supervised Prostate TMA Classification Via Graph Convolutional Networks," in 2020 IEEE 17th International Symposium on Biomedical Imaging (ISBI), Apr. 2019, pp. 239–243, DOI: <https://doi.org/10.1109/ISBI45749.2020.9098534>.
- [5] B. Patel, S. Sriprasad, J. Cadeddu, A. Thind, and A. Rane, "Obstacles in prostate cancer screening: Current issues and future solutions," vol. 12, no. 2, pp. 111–116, Nov. 2018, DOI: <https://doi.org/10.1177/2051415818815395>.
- [6] M. Xuru, "A Classification Method of Breast Pathological Image Based on Residual Learning," in Proceedings – 2020 International Conference on Computer Vision, Image and Deep Learning, CVIDL 2020, Jul. 2020, pp. 135–139, DOI: <https://doi.org/10.1109/CVIDL51233.2020.00033>.
- [7] R. Saturi and P. Prem Chand, "Implementation of Efficient Segmentation Method for Histopathological Images," in Proceedings of the 5th International Conference on Inventive Computation Technologies (ICICT 2020), Feb. 2020, pp. 419–423, DOI: <https://doi.org/10.1109/ICICT48043.2020.9112386>.
- [8] E. Cengiz, M. M. Kelek, Y. Oğuz, and C. Yılmaz, "Classification of breast cancer with deep learning from noisy images using wavelet transform," *Biomedizinische Technik*, vol. 67, no. 2, pp. 143–150, Apr. 2022, DOI: <https://doi.org/10.1515/BMT-2021-0163>.
- [9] S. Mehmood, T.M. Ghazal, M.A. Khan, M. Zubair, M.T. Naseem, T. Faiz and M. Ahmad, "Malignancy Detection in Lung and Colon Histopathology Images Using Transfer Learning With Class Selective Image Processing," *IEEE Access*, vol. 10, pp. 25657–25668, 2022. DOI: <https://doi.org/10.1109/ACCESS.2022.3150924>
- [10] U. K. Acharya and S. Kumar, "Genetic algorithm based adaptive histogram equalization (GAAHE) technique for medical image enhancement," *Optik (Stuttg)*, vol. 230, p. 166273, Mar. 2021, DOI: <https://doi.org/10.1016/J.JJLEO.2021.166273>.
- [11] F. A. Dzulkifli, M. Y. Mashor, and H. Jaafar, "Identification of Suitable Contrast Enhancement Technique for Improving the Quality of Astrocytoma Histopathological Images," *ELCVIA Electronic Letters on Computer Vision and Image Analysis*, vol. 20, no. 1, pp. 84–98, May 2021, DOI: <https://doi.org/10.5565/rev/elcvia.1256>.
- [12] S. Roy, A. Kumar Jain, S. Lal, and J. Kini, "A study about color normalization methods for histopathology images," *Micron*, vol. 114, pp. 42–61, Nov. 2018, DOI: <https://doi.org/10.1016/J.MICRON.2018.07.005>.
- [13] F. Bianconi, J. N. Kather, and C. C. Reyes-Aldasoro, "Experimental Assessment of Color Deconvolution and Color Normalization for Automated Classification of Histology Images Stained with Hematoxylin and Eosin," *Cancers*, vol. 12, no. 11, p. 3337, Nov. 2020, DOI: <https://doi.org/10.3390/CANCERS12113337>.
- [14] Ş. Öztürk and B. Akdemir, "Application of Feature Extraction and Classification Methods for Histopathological Image using GLCM, LBP, LBGLCM, GLRLM and SFTA," *Procedia Comput Sci*, vol. 132, pp. 40–46, Jan. 2018, DOI: <https://doi.org/10.1016/J.PROCS.2018.05.057>.
- [15] T. J. Alhindi, S. Kalra, K. H. Ng, A. Afrin, and H. R. Tizhoosh, "Comparing LBP, HOG and Deep Features for Classification of Histopathology Images," in Proceedings of the International Joint Conference on Neural Networks, Oct. 2018, DOI: <https://doi.org/10.1109/IJCNN.2018.8489329>.
- [16] S. Bhattacharjee, H. G. Park, C. H. Kim, D. P. Prakash, N. M. Madusanka, J. H. So, N. H. Cho, and H. K. Choi., "Quantitative Analysis of Benign and Malignant Tumors in Histopathology: Predicting Prostate Cancer Grading Using SVM," *Applied Sciences*, vol. 9, no. 15, p. 2969, Jul. 2019, DOI: <https://doi.org/10.3390/APP9152969>.
- [17] S. Sharma and R. Mehra, "Conventional Machine Learning and Deep Learning Approach for Multi-Classification of Breast Cancer Histopathology Images—a Comparative Insight," *J Digit Imaging*, vol. 33, no. 3, pp. 632–654, Jun. 2020, DOI: <https://doi.org/10.1007/S10278-019-00307-Y>.
- [18] D. Karimi, G. Nir, L. Fazli, P. C. Black, L. Goldenberg, and S. E. Salcudean, "Deep Learning-Based Gleason Grading of Prostate Cancer from Histopathology Images – Role of Multiscale Decision Aggregation and Data Augmentation," *IEEE J Biomed Health Inform*, vol. 24, no. 5, pp. 1413–1426, May 2020, DOI: <https://doi.org/10.1109/JBHI.2019.2944643>.
- [19] M. Gour, S. Jain, and U. Shankar, "Application of Deep Learning Techniques for Prostate Cancer Grading Using Histopathological Images," *Communications in Computer and Information Science*, vol. 1567, pp. 83–94, 2022, DOI: [https://doi.org/10.1007/978-3-031-11346-8\\_8](https://doi.org/10.1007/978-3-031-11346-8_8).
- [20] O. Kott, D. Linsley, A. Amin, A. Karagounis, C. Jeffers, D. Golijanin, T. Serre and B. Gershman, "Development of a Deep Learning Algorithm for the Histopathologic Diagnosis and Gleason Grading of Prostate Cancer Biopsies: A Pilot Study," *European Urology Focus*, vol. 7, no. 2, pp. 347–351, 2021. DOI: <https://doi.org/10.1016/j.euf.2019.11.003>
- [21] Y. Tolkach, T. Dohmgörge, M. Toma, and G. Kristiansen, "High-accuracy prostate cancer pathology using deep learning," *Nature Machine Intelligence*, vol. 2, no. 7, pp. 411–418, Jul. 2020, DOI: <https://doi.org/10.1038/s42256-020-0200-7>.
- [22] Y. Jusman, M. A. F. Nurkholid, and F. Utomo, "Prostate Image Classification Using Pretrained Models: GoogleNet and ResNet-50," in 2021 15th International Conference on Signal Processing

- and Communication Systems (ICSPCS 2021), 2021, DOI: <https://doi.org/10.1109/ICSPCS53099.2021.9660334>.
- [23] Q. A. Al-Hajja and A. Adebajo, "Breast cancer diagnosis in histopathological images using ResNet-50 convolutional neural network," in IEMTRONICS 2020 – International IOT, Electronics and Mechatronics Conference, Sep. 2020, DOI: <https://doi.org/10.1109/IEMTRONICS51293.2020.9216455>.
- [24] M. H. Motlagh, M. Jannesari, H. R. Aboulkheyr, P. Khosravi, O. Elemento, M. Totonchi, and I. Hajirasouliha., "Breast Cancer Histopathological Image Classification: A Deep Learning Approach," bioRxiv, p. 242818, Jan. 2018, DOI: <https://doi.org/10.1101/242818>.
- [25] F. Parvin and M. Al Mehedi Hasan, "A Comparative Study of Different Types of Convolutional Neural Networks for Breast Cancer Histopathological Image Classification," in 2020 IEEE Region 10 Symposium, TENSYPMP 2020, Jun. 2020, pp. 945–948, DOI: <https://doi.org/10.1109/TENSYPMP50017.2020.9230787>.
- [26] S. Bhattacharjee, H. G. Park, C. H. Kim, D. P. Prakash, N. M. Madusanka, J. H. So, N. H. Cho, and H. K. Choi., "Quantitative Analysis of Benign and Malignant Tumors in Histopathology: Predicting Prostate Cancer Grading Using SVM," Applied Sciences, vol. 9, no. 15, p. 2969, Jul. 2019, DOI: <https://doi.org/10.3390/APP9152969>.
- [27] M. A. Aswathy and M. Jagannath, "An SVM approach towards breast cancer classification from H&E-stained histopathology images based on integrated features," Med Biol Eng Comput, vol. 59, no. 9, pp. 1773–1783, Sep. 2021, DOI: <https://doi.org/10.1007/S11517-021-02403-0>.
- [28] A. Alqudah and A. M. Alqudah, "Sliding Window Based Support Vector Machine System for Classification of Breast Cancer Using Histopathological Microscopic Images," vol. 68, no. 1, pp. 59–67, 2019, DOI: <https://doi.org/10.1080/03772063.2019.1583610>.
- [29] S. Singh and R. Kumar, "Histopathological image analysis for breast cancer detection using cubic SVM," in 2020 7th International Conference on Signal Processing and Integrated Networks (SPIN 2020), Feb. 2020, pp. 498–503, DOI: <https://doi.org/10.1109/SPIN48934.2020.9071218>.
- [30] K. Lopez, M. Magboo, A. T.-B.- MLIS, and undefined, "A Clinical Decision Support Tool to Detect Invasive Ductal Carcinoma in Histopathological Images Using Support Vector Machines, Naïve-Bayes, and K-Nearest," vol. 332, pp. 46–53, Dec. 2020, DOI: <https://doi.org/10.3233/FAIA200765>.
- [31] R. Fogarty, D. Goldgof, L. Hall, A. Lopez, J. Johnson, M. Gadara, R. Stoyanova, S. Punnen, A. Pollack, J. Pow-Sang and Y. Balagurunathan, "Classifying Malignancy in Prostate Glandular Structures from Biopsy Scans with Deep Learning," *Cancers*, vol. 15, no. 8, pp. 2335, 2023. DOI: <https://doi.org/10.3390/cancers15082335>
- [32] R. Bazargani, W. Chen, S. Sadeghian, M. Asadi, J. Boschman, A. Darbandsari, A. Bashashati and S. Salcudean, "A novel H and E color augmentation for domain invariance classification of unannotated histopathology prostate cancer images," *Medical Imaging 2023: Digital and Computational Pathology*, pp. 35, 2023. DOI: <https://doi.org/10.1117/12.2654040>
- [33] M. Nishio, H. Matsuo, Y. Kurata, O. Sugiyama, and K. Fujimoto, "Label Distribution Learning for Automatic Cancer Grading of Histopathological Images of Prostate Cancer," *Cancers (Basel)*, vol. 15, no. 5, p. 1535, Mar. 2023, DOI: <https://doi.org/10.3390/CANCERS15051535>.
- [34] M. Koziarski, B. Cyganek, B. Olborski, Z. Antosz, M. Żydak, B. Kwolek, P. Wąsowicz, A. Buwała, J. Swadźba, P. Sitkowski., "DiagSet: a dataset for prostate cancer histopathological image classification," 2021. URL: <https://arxiv.org/abs/2105.04014v1> (Accessed: 23, Jun, 2023).